의학박사 학위논문

Heterodimerization of S310F HER2 Mutant with EGFR is Inhibited by Cetuximab, but not by Pertuzumab or Trastuzumab

S310F HER2 Mutant와 EGFR 이량체화는 Cetuximab에 의하여 저해되나, Pertuzumab과 Trastuzumab에 의하여 저해되지 않음

2020년 2월

서울대학교 대학원
의과학과의과학전공
신 정 원

A thesis of the Degree of Doctor Philosophy

S310F HER2 Mutant와 EGFR 이량체화는 Cetuximab에 의하여 저해되나, Pertuzumab과 Trastuzumab에 의하여 저해되지 않음

Heterodimerization of S310F HER2 Mutant with EGFR is Inhibited by Cetuximab, but not by Pertuzumab or Trastuzumab

February 2020

The Department of Biomedical Sciences,
Seoul National University
College of Medicine
Jungwon Shin

Abstract

G309 and S310 HER2 mutations are located in extracellular domain II region, which act as an epitope of pertuzumab and the dimerization arm. S310F, the most common mutation in the HER2 extracellular domain, can drive cancer without HER2 gene amplification. However, the effect of S310F mutation on the extracellular domain II poorly understood. In this study, the effects of G309 and S310 activating mutations on HER2 were evaluated using therapeutic antibodies and compared the dimerization of wild-type and S310F mutated HER2 with epidermal growth factor receptor (EGFR). G309A, G309E, S310F or S310Y mutations on HER2 resulted in the loss of binding activity of HER2 domain II binding antibody, pertuzumab, possibly due to structural change of HER2 domain II by the mutations. In addition, the phosphorylation of EGFR and HER2, and the viability of 5637 cells with S310F mutation were not affected by the pertuzumab. On the other hand, HER2 domain IV binding antibody, trastuzumab, still had binding activity to HER2 even in the presence of the mutations. However, as trastuzumab is a HER2 homodimerization blocking

antibody, it did not affect the phosphorylation and viabilityof 5637 cells. Surprisingly, phosphorylation of EGFR and HER2 and the viability of 5637 cells were affected by EGFR targeted antibody, cetuximab, and EGFR or pan-HER TKIs (tyrosine kinase inhibitor) such as gefitinib or lapatinib. Additionally, we confirmed EGFR/HER2 and EGFR/HER2 S310F heterodimerization levels were similar on EGFR and HER2 transfected cells. S310F missense mutation of HER2 is an activating mutation located on EGFR/HER2 dimerization arm. Even though the S310F mutation resulted in the structural change of HER2 domain II, the mutation did not affect the EGFR/HER2 heterodimerization. Therefore, EGFR/HER2 S310F heterodimerization was stillmainly formed in 5637 cell lines that are overexpressed with EGFR and harbor low levels of HER2 S310F mutation. For these results, we suggest the use of EGFR targeted antibodies or TKIs treatments for EGFR-overexpressed/low level HER2 S310F expressed cancer patients.

Keywords: HER2, Mutation, Pertuzumab, TIR microscope, EGFR, Heterodimerization

Student number: 2013-31177

Contents

List of Tables

List of Figures

List of Abbreviations

Cet: cetuximab

Tras: trastuzumab

Ptz: pertuzumab

Gef: gefitinib

Lap: lapatinib

ABTS : 2,2’ −azino−bis[3−ethylbenzothiazoline−6−sulphonic acid]

BSA: bovine serum albumin

C_K : kappa light chain constant region

ELISA : enzyme−linked immunosorbent assay

HRP : horseradish peroxidase

PBS : phosphate buffered saline

scFv : single chain fragment variable

TKI: tyrosine kinase inhibitor

Introduction

HER2/ErbB2/Neu is a member of the human epidermal growth factor receptor (EGFR, HER) family of homologous transmembrane receptor tyrosine kinases. The HER family is composed of four receptors (EGFR and HER2-4/ErbB1-4) and a number of variants generated by alternative slicing. There are 11 types of ligands reactive to HER family receptors, including those generated by alternative splicing[1]. The roles for these receptors and their ligands have been well described in many types of human cancers, including breast, colon, pancreatic, ovarian, brain, and lung cancers[2]. Binding of the ligand to EGFR or HER3/4 induces conformational changes in the proteins, facilitating receptor dimerization, which results in trans-phosphorylation oftyrosine residues in the carboxy tail[3]. The phosphortyrosines are docking sites for the recruitment of downstream signaling proteins. Human epidermal growth factor receptor 2 (HER2) has no known ligand but forms heterodimers with other EGFR family members and activates downstream signaling through the phosphoinositide 3-kinase/AKT and MAPK pathways[4].

Amplification/overexpression of HER2 is associated with cell transformation and oncogenesis[5], is observed in 20–25% of breast cancers, and is associated with poor survival[6]. In breast cancer cells with HER2 gene amplification, HER2 receptors exist on the cell surface as monomers, homodimers and heterodimers. The therapeutic antibody trastuzumab binds to extracellular domain IV and the epitope is P579–Q583, D592–F595 and K615–P625 residues. Trastuzumab cannot block ligand–induced HER2 heterodimers and has preferential activity against breast cancers driven by HER2 homodimers[7,8]. Meanwhile pertuzumab binds to extracellular domain II, D307–V308, L317–H318 and K336–P337 residues. This sterically blocks a binding pocket necessary for receptor dimerization, and inhibit HER2 association with its partner receptors[9]. This property may explain why pertuzumab, unlike trastuzumab, is effective against a broad range of cancers which do not express HER2 at high levels[10,11]. Antibody drug conjugates (trastuzumab emtansine), and small molecule tyrosine kinase inhibitors (lapatinib, erlotinib, and neratinib) have also dramatically improved the outcomes of HER2–positive cancer patients[12–15]. Besides the amplification/overexpression of HER2, somatic

HER2 gene mutations have been detected in a range of human cancer types, including prostate neuroendocrine cancer, metastatic cutaneous squamous cell carcinoma, and bladder cancer[16,17]. Preclinical data suggest that functionally activating HER2 mutations may drive and maintain cancers in a manner analogous to HER2 gene amplification and those HER2 mutations may similarly confer changes in sensitivity to HER2-directed drugs[18].

There are more than 20 extracellular domain mutations detected in human cancer tissues (Table 1)[8,18-37]. Furthermore, 26 additional extracellular domain mutations have been detected in various human cancer cell lines (Table 2). G309 and S310 mutations of HER2 domain II are well-known activating mutations. Previous studies showed that the G309 mutation leaves unpaired cysteine residues (C299-C311), forming reduction-sensitive dimmers[19]. Likewise, the S310 mutation promotes non-covalent dimerization between neighboring molecules, promoting hyperphosphorylation of HER2[19]. The NIH3T3 cells transfected with an expression vector encoding the S310F HER2 mutant were sensitive to trastuzumab, lapatinib, afatinib, and neratinib[19]. Clinically S310F is the most

frequently found mutation in the HER2 extracellular domain[38]. According to the cancer genomic cBioPortal database, S310F is the most commonly found mutation in the HER2 extracellular domain (0.4%)[39,40]. However,we did not find mutations in the genomic samples of Seoul National University Hospital.

Two HER2-nonamplified breast cancer patients with S310F mutation were successfully treated with the trastuzumab alone or in combination with pertuzumab[18,30]. G309 and S310 residues are located near the binding epitope for pertuzumab obscuring the reactivity of the antibody[9]. But the reactivity of pertuzumab as well as trastuzumab to the S310F mutant has not been previously reported. In this study, we prepared recombinant proteins corresponding to all reported G309 and S310 HER2 mutants and analyzed their interactions in Enzyme-linked immunosorbent assay (ELISA) with both trastuzumab and pertuzumab. We also used 5637 cells, an EGFR-amplified bladder cancer cell line expressing both S310F HER2 mutant and wild-type HER2 to analyze the downstream signaling of HER2 mutant and found that the S310F HER2 mutant efficiently formed heterodimers with EGFR, which could not be inhibited by trastuzumab as well as pertuzumab. And

using single molecule level total internal reflection (TIR) microscopy, we confirmed that S310F mutant can form a heterodimer with EGFR at the molecular level.

Table 1. HER2 extracellular domain mutations reported in previous studies from patient samples.

Protein change	Pfam domain[15]	Tumor type	Impact	HER2 gene amplification	Phosphorylation	Reference
L12R	-	Breast Cancer	ND	Negative	ND*	[34]
A20T		Lung cancer	ND	ND	ND	[23]
L49H		Lung cancer	ND	Negative	ND	[20]
L49H		Glioblastoma	ND	ND	ND	[19]
E139D	Receptor L	Breast Cancer	ND	Negative	ND	[34]
E139G		Breast Cancer	ND	Negative	ND	[34]
R157W		Bladder cancer (MPUC)	ND	Negative	ND	[31]
T216S	Furin-like	Lung cancer	ND	Negative	ND	[20]
T216S		Glioblastoma	ND	ND	High	[19]
I263T		Colorectal cancer	ND	Negative	ND	[35]
G309A		Breast Cancer	Activating	Negative	ND	[26]
G309E		Breast Cancer	Activating	Positive	ND	[23]
S310F		Gastric cancer	Activating	ND	High	[37]
S310F (2)		Breast Cancer		Negative	High	[25]
S310F		Lung cancer		Negative	High	[19]
S310F		Breast Cancer		Negative	High	[24]
S310F (2)		Colorectal cancer		Negative	High	[36]
S310F		Breast Cancer		Negative	High	[27]
S310F		Lung cancer		Positive	High	[21]
S310F		Breast Cancer		Negative	High	[28]
S310F (4)		Bladder cancer (MPUC)		Negative	High	[31]
S310F		Adnexal cancer		Negative	High	[32]

S310F	Furin-like	Breast Cancer	Activating	Negative	High	[28]
S310F (2)		Breast Cancer		Positive	High	[29]
S310F		Lung cancer		ND	High	[22]
S310F		Breast Cancer		Negative	High	[30]
S310F (4)		Breast Cancer		Positive	ND	[34]
S310Y		Lung cancer	Activating	ND	High	[23]
S310Y		Lung cancer		ND	High	[19]
S310Y		Colorectal cancer		Positive	High	[20]
S310Y		Bladder cancer (MPUC)		Negative	High	[19]
C311R and E321G		Lung cancer	ND	Negative	ND	[20]
C311R		Glioblastoma	ND	ND	Low	[19]
N319D		Lung cancer	ND	Negative	ND	[20]
N319D		Glioblastoma	ND	ND	ND	[19]
E321G		Glioblastoma	ND	ND	Low	[19]
D326G and C334S		Lung cancer	ND	Negative	ND	[20]
D326G		Glioblastoma	ND	ND	Low	[19]
C334S		Glioblastoma	ND	ND	ND	[19]
A466T	Receptor L	Colorectal cancer	ND	Negative	ND	[35]
A466V		Breast Cancer	Activating	Negative	High	[34]
C515R	Growth factor receptor	Breast Cancer	Activating	Negative	High	[34]
T526A		Breast Cancer	Activating	Negative	High	[34]

* ND = no data available

Table 2. HER2 extracellular domain mutations reported in cell lines.

Cell line	Protein change	Pfam domain[15]	Lineage	Impact	phosphorylation
SW1271	S22N	-	Lung	ND*	ND
HEC59	R100W	Receptor L	Endometrium	ND	ND
HEC108	T166M		Endometrium	ND	ND
SBC1	Q178H		Lung	ND	ND
MOLT16	R217H	Furin-like	Haematopoietic and lymphoid tissue	ND	ND
NALM6	R226H		Haematopoietic and lymphoid tissue	ND	ND
KM12	P230L		Large intestine	ND	ND
DSH1	D277H		Urinary	ND	ND
5637	S310F		Urinary	Activating	High
DSH1			Urinary		
OACM51			Oesophagus		
HRT18	L313I		Intestine	ND	ND
NCIH2110	N319Y		Lung	ND	ND
HCC1359	T328S		Lung	ND	ND
NCIH1563	S335C		Lung	ND	ND

Jurkat	S335I	-	Haematopoietic and lymphoid tissue	ND	ND
OC314	A386T	Receptor L	Ovary	ND	ND
OC316	A386T		Ovary	ND	ND
NCIN87	F425L		Stomach	ND	ND
NCIN87	L436V		Stomach	ND	ND
SET2	T444S		Haematopoietic and lymphoid tissue	ND	ND
M059J	W452S		Central nervous system	ND	ND
Jurkat	T479M		Haematopoietic and lymphoid tissue	ND	ND
ISTSL1	R499Q	-	Lung	ND	ND
SUPB8	R499W		Haematopoietic and lymphoid tissue	ND	ND
RL952	G518V	Growth factor receptor	Endometrium	ND	ND
NCIH1793	V541M		Lung	ND	ND
NCIH740	R558M		Lung	ND	ND
Karpas45	A586G		Haematopoietic and lymphoid tissue	ND	ND

* ND = no data available

Materials and Methods

1. Expression and purification of recombinant fusion proteins

Genes encoding the extracellular domain of wild-type HER2, wild-type HER3 and G309A, G309E, S310F, or S310Y HER2 mutants were chemically synthesized with *Sfi*I restriction sites at the 5′ and 3′ ends (GenScript Biotech, Jiangsu, China). After restriction digestion with *Sfi*I (New England Biolabs, Hertfordshire, UK), the genes were ligated into pCEP4 vectors encoding either human Fc or Cκ, as described previously[41,42]. Genes encoding the scFv form of pertuzumab, trastuzumab, and cetuximab were also synthesized with *Sfi*I restriction sites at the 5′ and 3′ ends (GenScript Biotech) and cloned into the human Cκ vector[43-45].

The expression vectors were then transfected into HEK293F cells (FreeStyle 293-F cells) using polyethylenimine (Sigma-Aldrich, St. Louis, MO, USA) as described previously[46]. The transfected cells were grown in FreeStyle 293 expression media (Invitrogen, Carlsbad, CA, USA) as described

previously[47]. The culture supernatants were purified by affinity chromatography using either Protein A or KappaSelect resin (GE Healthcare, Buckinghamshire, UK) following the manufacturer's instructions.

The purified recombinant proteins were subjected to 4-12% NuPage bis-Tris gels (Invitrogen) according to the manufacturer's instructions. After the electrophoresis, the gel was stained with Coomassie Brilliant Blue R-250 (Ameresco, Framingham, MA, USA).

2. ELISA

Recombinant wild-type HER2, wild-type HER3 or HER2 mutant extracellular domain-human Fc fusion proteins were coated overnight at 4° C on the wells of microtiter plates (Corning, Corning, NY, USA). The wells were blocked with 130 μL of blocking buffer [3% bovine serum albumin (BSA) in phosphate-buffered saline (PBS)] for 1 h at 37° C. The plates were then incubated with recombinant pertuzumab or trastuzumab scFv- human Cκ fusion proteins serially diluted four-fold in blocking buffer for 2 h at 37° C. The plates were then washed with 150 μL of 0.05% Tween 20 in PBS (PBST)

for three times. Subsequently, horseradish peroxidase (HRP) conjugated anti-human Cκ light chain antibody(1:5,000; Millipore, Hayward, CA, USA) was added to each well. After incubation for 1 h at 37° C, the plates were washed. Finally, 50 μL of 3,3′,5,5′-tetramethylbenzidine substrate solution (TMB) substrate was added and optical density was measured at 650 nm (LabSystems Diagnostics Oy, Vantaa, Finland).

3. Cell culture

The 5637and AU565 cells were obtained from the Korean Cell Line Bank (Seoul, Republic of Korea). The cells were grown in RPMI-1640 media (Welgene, Seoul, Republic of Korea) supplemented with 10% fetal bovine serum (Thermo Fisher Scientific, Gibco, Waltham, MA, USA) and 1% penicillin-streptomycin (1,000 U/mL) (Thermo Fisher Scientific, Gibco).

4. Sequencing of amplified HER2 gene fragments of5637cell

Total RNA was isolated from the 5637 cells using TRIzol reagent (Invitrogen) as previously described[48]. After

cDNA was synthesized using a SuperScript III First-Strand Synthesis system (Invitrogen), the HER2 gene fragment encoding from N302 residue to R340 residue was amplified using specific primer sets (HER2 forward: 5′-GCCTCCACTTCAACCACAGTGGC-3′ and HER2 reverse: 5′-CTGTGATCTCTTCCAGAGTCTCAAAC-3′). The PCR conditions were as follows: preliminary denaturation at 95° C for 7 min, followed by 25 cycles of 30 s at 95° C, 30 s at 54° C, and 1 min at 72° C. The reaction was ended with an extension step for 5 min at 72° C.After agarose gel electrophoresis, the amplified DNA was extracted using the Qiagen Gel Extraction Kit according to the manufacturer's instructions (Qiagen, Hilden, Germany) and subjected to Sanger sequencing (Macrogen, Seoul, Republic of Korea).

5. Flow cytometry analysis

The 5637 and AU565 cells (3×10^5 cells/well, Corning) were resuspended in 100 μL of flow cytometry buffer (1% BSA and 0.02% sodium azide in PBS), then incubated with cetuximab, pertuzumab, or trastuzumab scFv- human Cκ fusion proteins at a final concentration of 1 μM for 1 h at 37° C. The cells

were then washed twice with 1% (w/v) BSA in PBS and incubated with FITC-conjugated anti-human κ light chain antibody (Thermo Fisher Scientific) for 40 min at 37° C. After washing with flow cytometry buffer, the fluorescence intensity of cells was measured using a FACS Canto II (BD Bioscience, Heidelberg, Germany) and analyzed with FlowJo data analysis software (Threestar, OR, USA). Non-transfected HEK293T cell and cells transfected with EGFR-mCherry and HER2-eGFP bicistronic expression vector were used as control cells and were analyzed in the same manner as above.

6. Immunoprecipitation and immunoblot analyses

The AU565 and 5637 cells (1×10^7 cells) were lysed in 100 μL of cold RIPA buffer (150 mM NaCl, 1% Triton X-100, 1% sodium deoxycholate, 0.1% sodium dodecyl sulfate, 50 mM Tris-HCl, and 2 mM EDTA at pH 7.5) containing a protease inhibitor cocktail (Roche, Basel, Switzerland). Subsequently, 500 μL of the cell lysatewas incubated with either recombinant trastuzumab or pertuzumab scFv-human C κ fusion protein with a final concentration of 100 μg/mL at 4° C overnight with rotation. Then, 10 μL of KappaSelect resin

(GE Healthcare) was added to the lysate, followed by incubation at 4° C for 4 h with gentle rotations. After centrifugation for 3 min at 1,200 × *g*, the resin and supernatant were collected. The cell lysate, resin, and supernatant representing the same number of the cells were subjected to SDS-polyacrylamide gel electrophoresis (SDS-PAGE)as described above and transferred onto nitrocellulose membranes (Whatman, Dassel, Germany) using a transfer system as previously described[49]. Thereafter, the membrane was blocked with 5% skim milk (BD Biosciences, CA, USA) followed by incubation with rabbit anti-HER2 antibody (Cell Signaling Technology, Danvers, MA, USA) at 4° Covernight and with horseradish peroxidase (HRP)-conjugated goat anti-rabbit IgG (1:5,000, 111-035-008; Jackson ImmunoResearch Laboratory, West Grove, PA, USA). After several washes with Tris-buffered saline and Tween [10 mM Tris-HCl, pH 7.5, 150 mM NaCl, and 1% (v/v) Tween 20], the protein bands were visualized using Super Signal Pico West chemiluminescent substrate (#34080; Thermo Fisher Scientific) and a gel doc EZ system (Bio-Rad, Hercules, CA, USA).

7. Cell viability assay and immunoblotting

The 5637 cells were seeded at a density of 5.5–10 × 10^3/well in 96-well culture plates. After incubation for 24 h, cells were treated with 1 μM of cetuximab (Merck, Palo Alto, CA, USA), pertuzumab (Roche), trastuzumab (Roche), gefitinib (AstraZeneca, Cambridge, UK), or lapatinib (GlaxoSmithKline, Brentford, UK). After 96 h, the number of viable cells was determinedusing a Premix WST-1 kit (Takara, Kyoto, Japan) following the manufacturer ' s protocol. For immunoblot analysis, 5637 cells were lysed in ice-cold RIPA buffer containing a protease inhibitor cocktail (Roche) and phosphatase inhibitor (Roche). The cell lysates were cleared by centrifugation for 10 min at 13,000 × *g* and the amount of protein in the supernatants was determined by a BCA assay (Pierce Biotechnology, Waltham, MA, USA). The proteins in the supernatants were separated by SDS-PAGE using 4–12% bis-Tris gels (Invitrogen) as described aboveand transferred onto a nitrocellulose membrane. The membrane was blocked by preincubation in 5% BSA/0.2% TBST at room temperature for 30 min and then incubated with anti-EGFR antibody (Cell Signaling Technology), anti-phospho-EGFR (Tyr 1068)

antibody (Cell Signaling Technology), anti-HER2 antibody (Cell Signaling Technology), anti-phospho-HER2 (Tyr 1221/1222) antibody (Cell Signaling Technology), anti-PARP (Cell Signaling Technology), anti-cleaved PARP (Cell Signaling Technology), or anti-β-actin antibody (Cell Signaling Technology) for overnight at 4° C. After washing three times with 0.2% TBST, the membrane was incubated with either HRP-conjugated goat anti-rabbit IgG Fc antibody (#31463; Thermo Fisher Scientific) or HRP-conjugated goat anti-mouse IgG antibody (sc-2005; Santa Cruz Biotechnology, Santa Cruz, CA, USA) for 1 h at room temperature. The membrane was washed three times with TBST, and the bound antibody was visualized by addition of SuperSignal Pico West chemiluminescent substrate (#34080; Thermo Fisher Scientific) following the manufacturer's instructions. The Image Lab program (Biolab) was used to determine the intensity of bands.

8. Single-molecular interaction analysis using total internal reflection fluorescence (TIRF) microscopy

Single-molecular interaction analysis was performed as described in a previous study with appropriate modifications[50].

Genes encoding fusion proteins composed of the extracellular domain of the EGFR fused with mCherry protein (EGFR-mCherry) and that of wild-type HER2 fused with eGFP (HER2-eGFP)were ligated into a bicistronic expression vector. Another expression vector was prepared with the S310F mutant (S310F HER2-eGFP) replacing wild-type HER2. Then, these vectors were transfected into HEK293T cells (FreeStyle 293-T cells). After culture at 37° C with 5% CO_2 for 1 day, the cells were dissolved in lysis buffer (1% Triton X-100, 150 mM NaCl, 1 mM EDTA, 10% glycerol) with protease (P8340; Sigma-Aldrich) and phosphatase (P5726; Sigma-Aldrich) inhibitor cocktail. After centrifugation at 15,000 × *g* for 10 min at 4° C, the supernatant was collected. Recombinant mCherry (4999-100; Biovision, Milpitas, CA, USA) and eGFP (4993-100; Biovision) protein standards were used to determine the concentration of fluorescently tagged proteins in the cell lysates. The fluorescence levels for recombinant eGFP and mCherry proteins of known concentrations (5-25 nM, five different concentration points) were measured using a fluorometer (Enspire 2300; Perkin-Elmer, San Jose, CA, USA) and were used to construct a calibration curve.

Detailed procedures of the flow chamber construction are described in previous studies[51,52]. The flow chamber was washed twice with 200 μL of PBS. Afterwards, 50 μL of NeutrAvidin solution(A2666; Invitrogen) was added to the flow chamber and was incubated for 5 min at room temperature. Subsequently, the flow chambers were washed twice followed by addition of diluted biotinylated polyclonal RFP antibody (34771; Abcam, Cambridge, UK) for 5 min at room temperature. This antibody was reported to be reactive to all RFP variants from *Discosoma,* including mCherry. After the flow chambers were washed again, cell lysates were added and incubated for 10 min at room temperature. Finally, the flow chambers were washed with 0.1% lysis buffer/PBS. EGFR/HER2 heterodimers were then detected with a TIRF microscope equipped with a 488-nm laser for eGFP detection. The images were recorded at 0.1 sec per frame, and 20 frames were recorded. To obtain a time-averaged image,three frames were averaged. EGFP spots were characterized from these time-averaged images. To obtain the intensity of eGFP spots, 10 time-averaged images were used.

Results

1. The recombinant S310F mutant is not reactive to pertuzumab but binds to trastuzumab.

A construct encoding the S310F HER2 extracellular domain fused to a human Fc domain of immunoglobulin heavy chain was prepared and cloned into a mammalian expression vector. For comparison, the expression vectors encoding the extracellular domains of all the other G309 and S310 mutants reported previously (G309A, G309E, S310F and S310Y HER2 mutants) and those of wild-type HER2 and HER3 were also prepared. After transfection, the recombinant fusion proteins were purified from the culture supernatant using an affinity column reactive to human Fc. The extracellular domain of four mutants and wild-type HER2 was also prepared as a fusion protein of human Cκ through cloning into a mammalian expression vector, transfection and purification using an affinity column reactive to human Cκ from the culture supernatant. To check the purity, the recombinant fusion proteins were subjected to SDS-polyacrylamide gel electrophoresis and the

gel was stained. No band except the fusion protein was visualized. In non-reducing conditions, multimers of G309E HER2 mutant fusion proteins were visualized in both fusion protein forms (Figure 1). The purified recombinant Fc fusion proteins were then subjected to an ELISA to test reactivity to pertuzumab and trastuzumab (Figure 2). A microtiter plate was coated with the recombinant Fc fusion proteins, blocked, and incubated with either pertuzumab or trastuzumab expressed as recombinant scFv-human Cκ fusion protein. Then, the amount of bound antibody was determined using anti-human Cκ antibody conjugated to HRP. S310F mutants did not bind to pertuzumab but reacted with trastuzumab in a dose-dependent manner (Figure 3). Pertuzumab did not bind to the G309E, S310F, and S310Y HER2 mutants, but reacted with the S309A HER2 mutant with reduced affinity compared to that of the wild-type HER2. Trastuzumab bound to the wild-type HER2 and all G309 and S310 HER2 mutants in a dose-dependent manner.

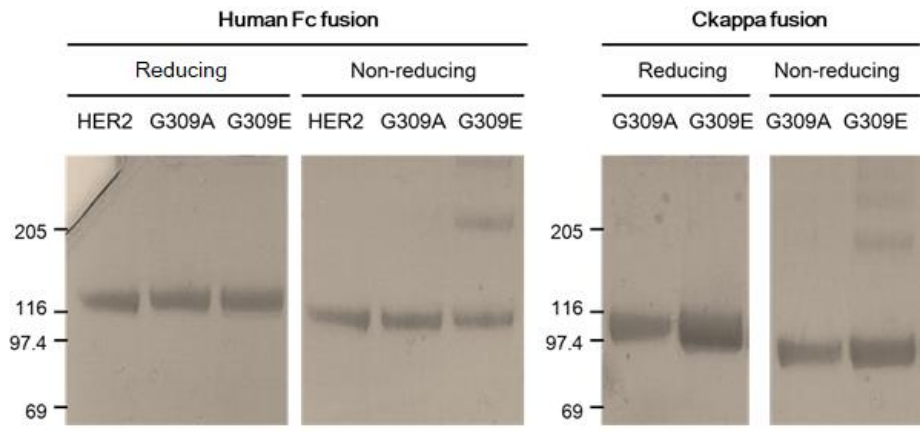

Figure 1. SDS-polyacrylamide gel electrophoresis analysis of recombinant G309 mutant extracellular domains fused with the human Fc or Cκ domain. The expression vectors encoding the fusion proteins were transfected into HEK293F cells. The recombinant proteins were purified from the culture supernatants using the affinity resin reactive to either Fc or human Cκ and subjected to 4%-12% (w/v) SDS-polyacrylamide gel electrophoresis either with or without a reducing agent. After electrophoresis, the protein bands were visualized with Coomassie Blue staining.

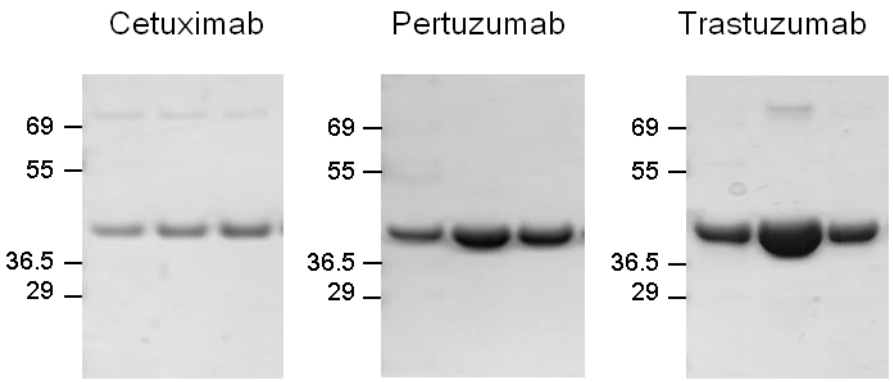

Figure 2. Expression of recombinant anti-EGFR family antibodies. The human Cκ fusion anti-EGFR family antibodies were expressed in HEK293F cells and confirmed by polyacrylamide gel electrophoresis.

a

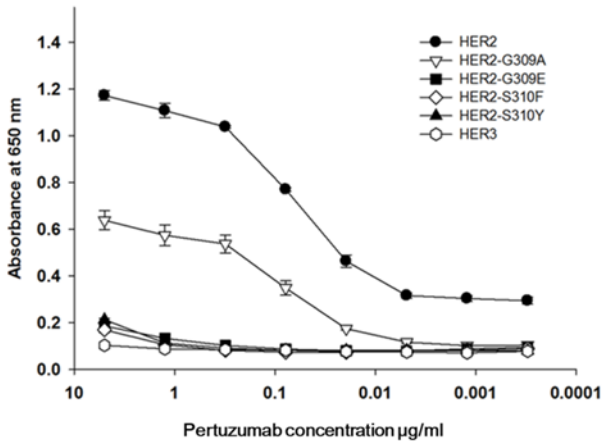
HER2
HER2-G309A
HER2-G309E
HER2-S310F
HER2-S310Y
HER3
Absorbance at 650 nm
1.4
1.2
1.0
0.8
0.6
0.4
0.2
0.0
10
1
0.1
0.01
0.001
0.0001
Pertuzumab concentration µg/ml

b

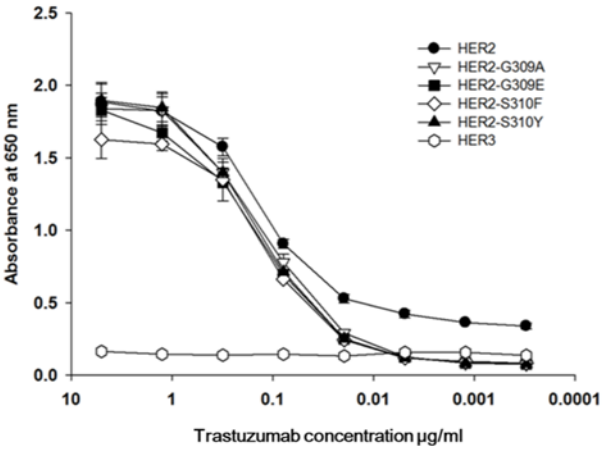
HER2
HER2-G309A
HER2-G309E
HER2-S310F
HER2-S310Y
HER3
Absorbance at 650 nm
2.5
2.0
1.5
1.0
0.5
0.0
10
1
0.1
0.01
0.001
0.0001
Trastuzumab concentration µg/ml

Figure 3. Reactivity of G309 and S310 HER2 mutants to pertuzumab and trastuzumab. Recombinant G309 and S310 mutant, wild-type HER2, or wild-type HER3 human Fc fusion protein was coated onto the wells of microtiter plates. The plate was blocked and subjected to incubation with (a) recombinant pertuzumab scFv-human Cκ fusion protein, or (b) trastuzumab scFv-human Cκ fusion protein at varying concentrations. Wild-type HER3 human Fc fusion protein was used as a negative control, because it does not bind to either antibody. The amount of bound antibody was determined using HRP-conjugated human Cκ light chain antibody and 3,3′,5,5′-tetramethylbenzidine (TMB) substrate solution

2. A bladder cancer cell line, 5637, expresses both wild-type HER2 and S310F mutant.

We searched literatures to identify a human cell line expressing the S310F mutant and found that bladder cancer cell line 5637 expressed the mutant. To test the allelic expression of the S310F HER2 mutant in the 5637 cell line, we extracted total RNA from the cells and prepared cDNA. A HER2 gene fragment including the S310 residue was amplified by PCR using specific primers and subjected to Sanger sequencing. A representative sequence chromatogram is shown in Fig. 2. We found that both the wild-type (nucleotide C) and the mutant (nucleotide T) peaks co-existed at the corresponding nucleotide position (Figure 4). To check the expression of the wild-type and mutant HER2 on the cell surface, we used recombinant trastuzumab and pertuzumab scFv-Cκ fusion proteins to avoid the possible non-specific interaction through Fc regions of IgG and Fc receptors on the cell and performed flow cytometric analyses. As expected, pertuzumab as well as the trastuzumab scFv-Cκ fusion protein reacted with the 5637 cells (Figure 5), which proved the presence of the wild-type HER2 on the cell surface of 5637 cells.

To confirm the expression of the S310F HER2 mutant in 5637 cells, we used immunoprecipitation experiments. We hypothesized that if the cells expressed the S310F HER2 mutant, it would not be immunoprecipitated by pertuzumab and would remain in the cell lysate. To determine the saturable amount of pertuzumab for immunoprecipitation experiments, we screened cell lines expressing higher amounts of HER2 than 5637 cells and identified AU565 cells (Figure 5). The amount of pertuzumab and trastuzumab scFv-Cκ fusion protein guaranteeing the immunoprecipitation of all of HER2 in AU565 cell lysates was then determined (Figure 6). This predetermined amount of scFv-human Cκ fusion protein was then incubated with the 5637 cell lysate, with added affinity resin reactive to Cκ. After centrifugation, pellets and supernatants were collected. Thereafter, the cell lysate, precipitated resin, and supernatant representing the same number of 5637 cells were subjected to SDS-polyacrylamide gel electrophoresis and immunoblot analysis using anti-HER2 antibody reactive to the HER2 domain III. Trastuzumab scFv-Cκ fusion protein immunoprecipitated nearly all HER2 molecules in the 5637 cell lysate, but pertuzumab scFv-human Cκ fusion

protein immunoprecipitated only a fraction of HER2 (Figure 6). With this observation, we concluded that 5637 cells expressed significant amounts theS310F mutant.

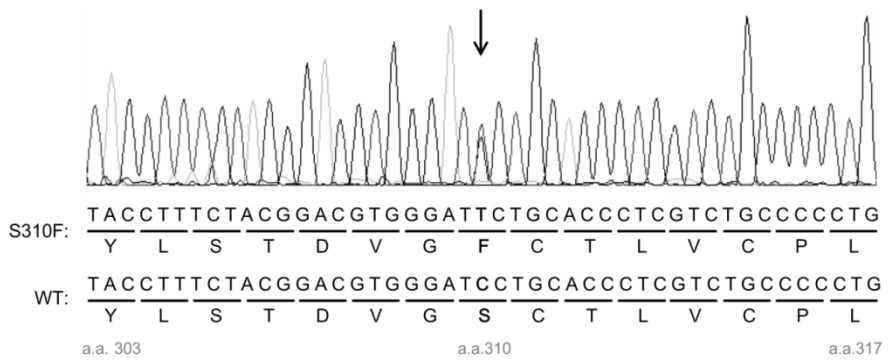

Figure 4. Sanger sequencing of 5637 cell HER2 gene. A representative sequence chromatogram showing the presence of two transcripts encoding wild-type HER2 and the S310F mutant in 5637 cells.

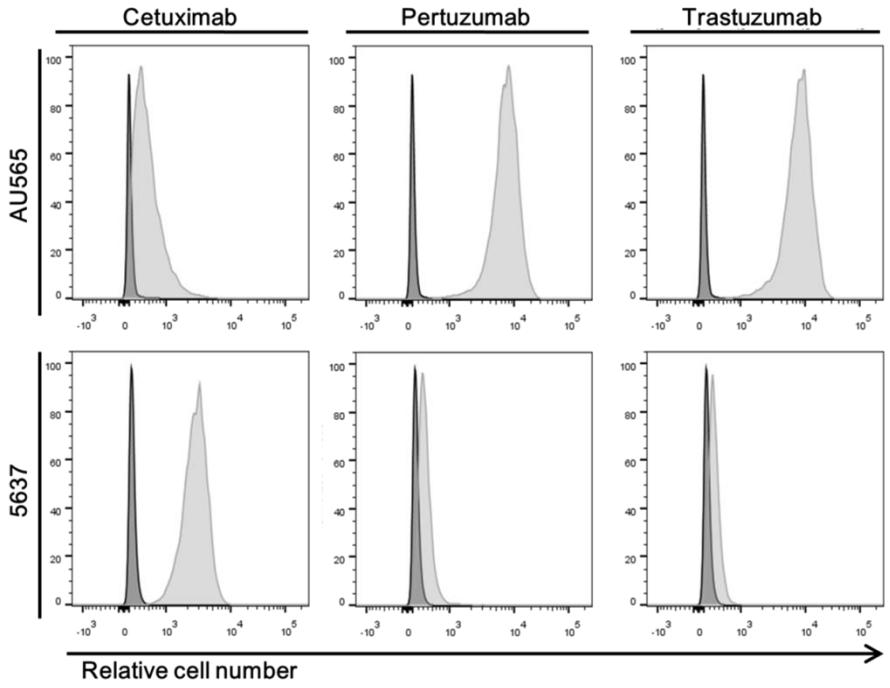

Figure 5. Expression of HER2 and EGFR in 5637 and AU565 cells. Flow cytometry analysis of two cancer cell lines assessing their reactivity to cetuximab, pertuzumab, and trastuzumab. The cells were incubated with individual antibody using the recombinant scFv-human Cκ fusion protein. The amount of bound antibody was determined using Allophycocyanin (APC)-labeled anti-human Cκ antibody.

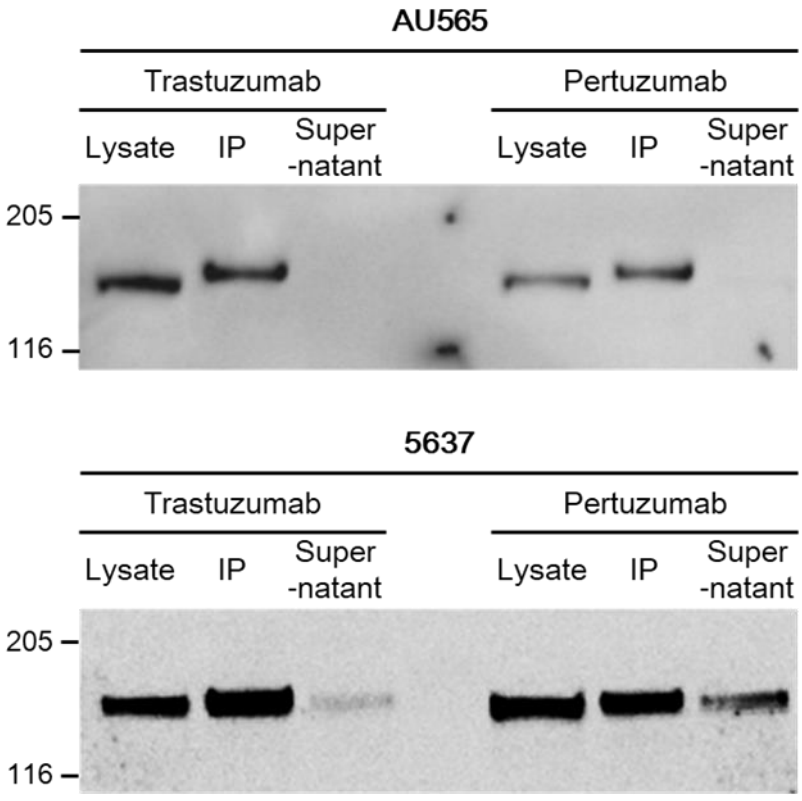

Figure 6. Immunoprecipitations of HER2 in AU565 and 5637 cell lysates using trastuzumab and pertuzumab. Cell lysates were incubated with trastuzumab or pertuzumab scFv− human Cκ fusion protein followed by affinity resin reactive to human kappa light chain. After centrifugation, the amount of HER2 in the supernatant, resin, and cell lysate representing the same number of cells was determined by immunoblot analysis using anti−HER2 antibody.

* IP = Immunoprecipitated

3. EGFR activates S310F HER2 mutant in 5637 cell.

We tested the effects of anti-HER2 agents on 5637 cell proliferation and the level of HER2 phosphorylation at Y1221 and Y1222 residues. The cells were incubated with pertuzumab, trastuzumab and lapatinib for 96 h, lysed and subjected to SDS-PAGE and immunoblot analysis using anti-phospho-HER2 antibody. In parallel, the number of viable cells after the incubation was determined. Inhibiting the ligand-independent dimerization of wild-type and S310F HER2 mutant by trastuzumab did not reduce the cell proliferation or HER2 phosphorylation(Figure 7, 8, 9). Inhibiting the ligand-dependent dimerization of wild-type HER2 by pertuzumab also failed to show any effect (Figure 7, 8, 9). However, lapatinib inhibited the cell proliferation and reduced HER2 phosphorylation (Figure 7, 8, 9(b)). Because lapatinib inhibits the catalytic activity of both the EGFR and HER2, we then tested the effects of cetuximab and gefitinib, and both effectively inhibited the cell proliferation and reduced the levels of phosphorylated HER2and EGFR (Figure 7, 8, 9). The apoptosis induced by anti-EGFR and anti-HER2 agents was

also determined (Figure 8, 9(b)). In accordance with the cell proliferation data, only cetuximab, gefitinib, and lapatinib induced the cleavage of PARP (Figure 8, 9(c)). Based on these data, we concluded that EGFR induced phosphorylation of S310F mutant in 5637 cells.

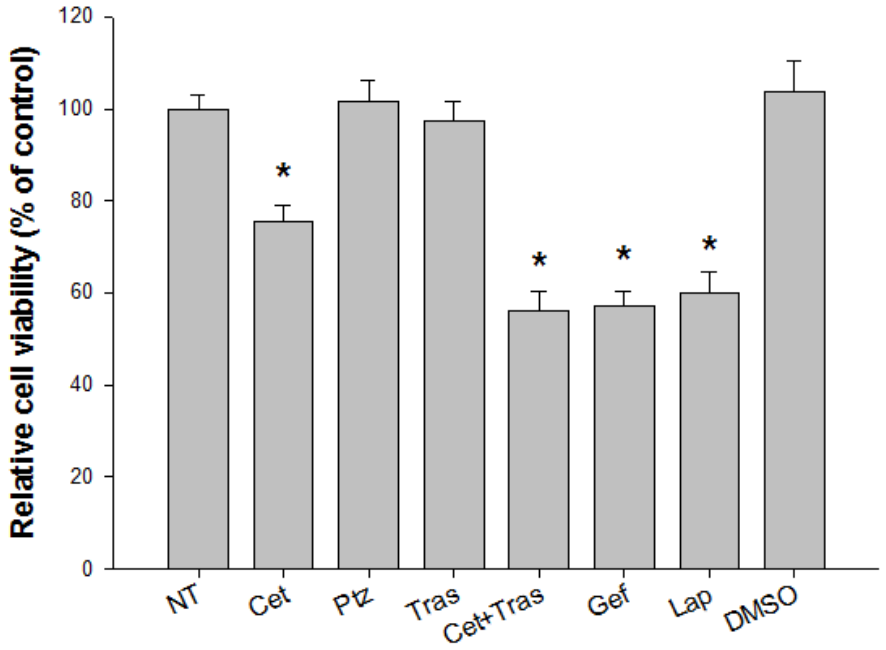

Figure 7. Cell growth inhibition by anti-HER2 and anti-EGFR agents. Cells were treated with HER2 or EGFR inhibitors for 96 h. Cell viability was measured by WST-1 kit as described in materials and methods. Relative cell viability as a percent was determined as ((absorbance in each treatment set - absorbance in untreated set) / absorbance in non-treated set X 100). Results represent the mean ± SD obtained from experiments performed in three independent experiments. NT; not treated, Cet; Cetuximab, Ptz; Pertuzumab, Gef; Gefitinib, Lap; Lapatinib, DMSO; dimethyl sulfoxide, PARP; poly (ADP-ribose) polymerase.

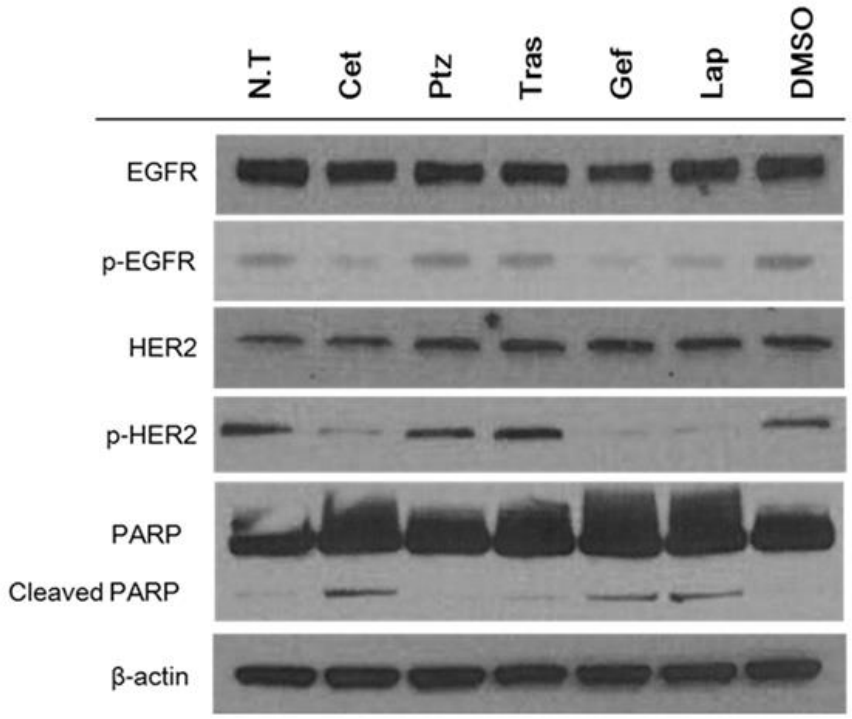

Figure 8. Inhibition of 5637 cell proliferation and receptor activation by anti-HER2 and anti-EGFR agents. Cells were treated with HER2 or EGFR inhibitors for 96 h. The cell lysate was subjected to immunoblot analysis to visualize the relative phosphorylation level of EGFR and HER2 and the level of cleaved PARP. NT; not treated, Cet; Cetuximab, Ptz; Pertuzumab, Gef; Gefitinib, Lap; Lapatinib, DMSO; dimethyl sulfoxide, PARP; poly (ADP-ribose) polymerase.

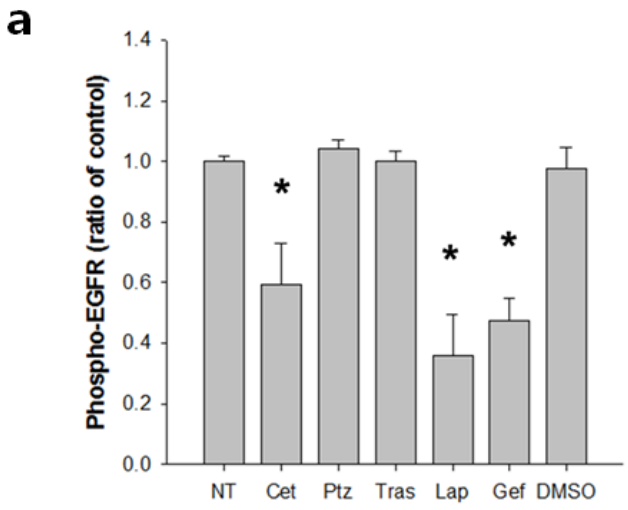
a
Phospho-EGFR (ratio of control)
1.4
1.2
1.0
0.8
0.6
0.4
0.2
0.0
*
*
*
NT
Cet
Ptz
Tras
Lap
Gef
DMSO

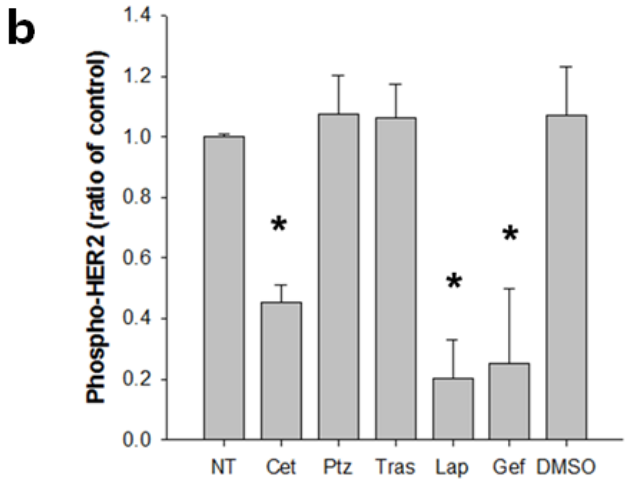
b
Phospho-HER2 (ratio of control)
1.4
1.2
1.0
0.8
0.6
0.4
0.2
0.0
*
*
*
NT
Cet
Ptz
Tras
Lap
Gef
DMSO

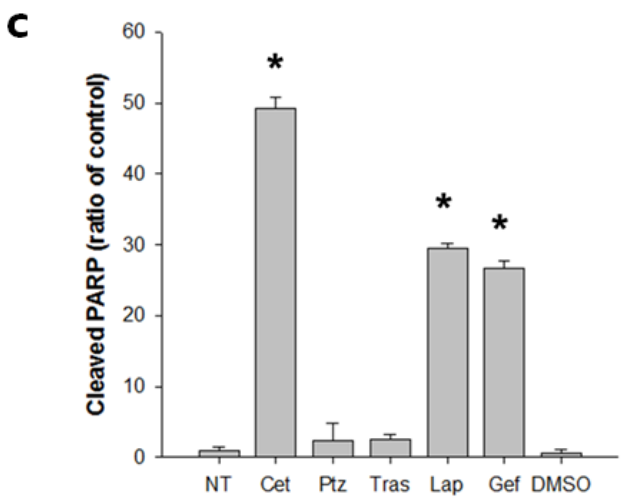
c
Cleaved PARP (ratio of control)
60
50
40
30
20
10
0
*
*
*
NT
Cet
Ptz
Tras
Lap
Gef
DMSO

Figure 9. Relative phosphorylation level of EGFR (a) and HER2 (b) and the level of cleaved PARP (c). Each these levels of figure 8 were quantified by densitometry and plotted, individually. *P < 0.005. NT; not treated, Cet; Cetuximab, Ptz; Pertuzumab, Gef; Gefitinib, Lap; Lapatinib, DMSO; dimethyl sulfoxide, PARP; poly (ADP−ribose) polymerase.

4. Single-molecular interaction analysis demonstrated that he S310F HER2 mutant formed heterodimers with the EGFR.

Single molecule interaction analysis was performed to determine whether the HER2 S310F mutant formed a heterodimer with the EGFR. We constructed a bicistronic mammalian expression vector encoding EGFR-mCherry and HER2 S310F-eGFP fusion proteins. For comparison, we also prepared another expression vector encoding EGFR-mCherry and wild-type HER2-eGFP fusion proteins. After transfection of the expression vector into HEK293T cells, the expression of EGFR, HER2 S310F mutant, and wild-type HER2 were confirmed by flow cytometry analysis; using recombinant cetuximab, trastuzumab and pertuzumab scFv-human Cκ fusion proteins, the HEK293T cells showed basal expression of EGFR and HER2 (Figure 10). The transfected cells showed significantly increased reactivity to cetuximab and trastuzumab. In HEK293T cells transfected with the expression vector encoding EGFR-mCherry and HER2 S310F-eGFP, the reactivity with pertuzumab was significantly lower compared to

the cells transfected with that encoding EGFR-mCherry and wild-type HER2-eGFP.

After transfection, the cells were allowed to grow for 24 h and then lysed. The level of EGFR-mCherry and wild-type and HER2 S310F-eGFP in the cell lysate was determined by measuring the fluorescence intensity. After a calibration curve was prepared using recombinant mCherry and eGFP protein standard with a florometer, the ratios of EGFR-mCherry vs wild-type HER2-eGFP and EGFR-mCherry vs HER2 S310F-eGFP in the cell lysates were determined to be 1:2.14 and 1:2.98, respectively. For single molecule interaction analysis, the lysate was subjected to a flow chamber coated with anti-mCherry antibody. Using the TIRF microscope, eGFP spots were identified and their intensity was determined and summed. The eGFP spot intensity summation value was increased in a dose-dependent manner as the concentration of EGFR-mCherry injected into the flow cell was increased in both the cell lysates of wild-type HER2-eGFP and HER2 S310F-eGFP transfectants (Figure 11). Considering the ratio of wild-type HER2-eGFP and HER2 S310F-eGFP vs EGFR-mCherry in the cell lysates of the two transfectants, the ratio of eGFP vs

mCherry in the HER2 S310F-eGFP transfectants was not significantly different from that of the wild-type HER2-eGFP transfectants (Figure 11). Two additional independent experiments yielded similar results. Based on these observations, we concluded that HER2 S310F interacted with the EGFR and its efficiency was comparable to that of the EGFR and wild-type HER2 interactions.

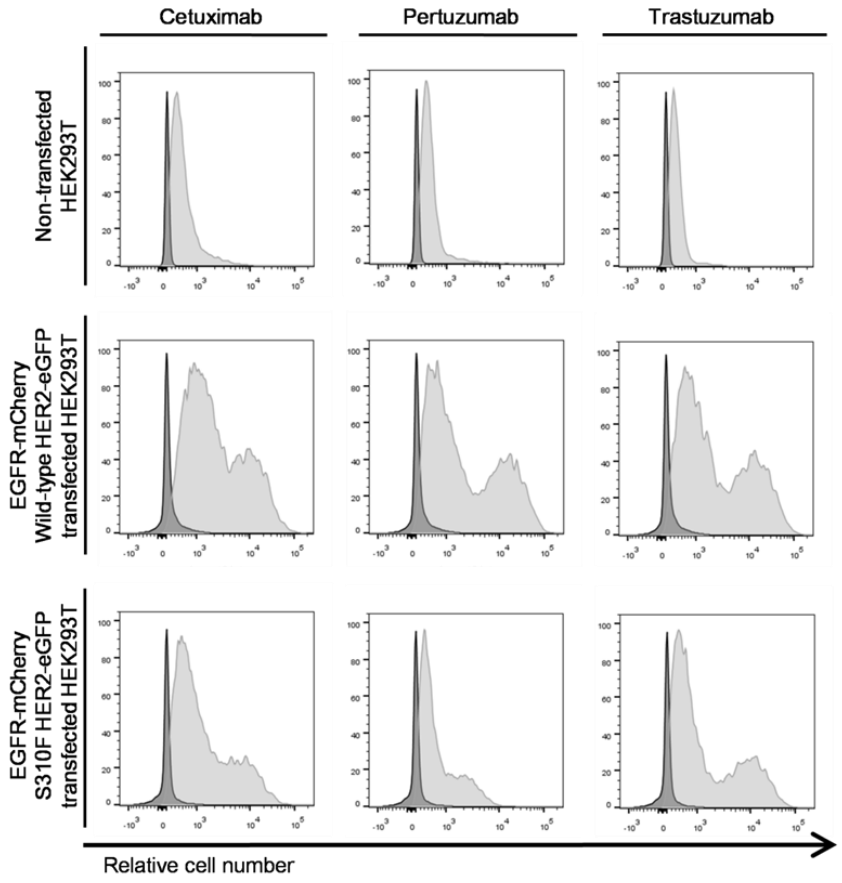

Figure 10. Bicistronic vector transfection which encoding either EGFR-mCherry and wild-type HER2-eGFP or EGFR-mCherry and S310F HER2-eGFP fusion proteins into HEK293T cell. After transfection, the cell surface expression of EGFR and HER2 or HER2 was checked by flow cytometry analysis using cetuximab, pertuzumab, and trastuzumab in the scFv-human Cκ format and APC-labeled anti-human Cκ antibody

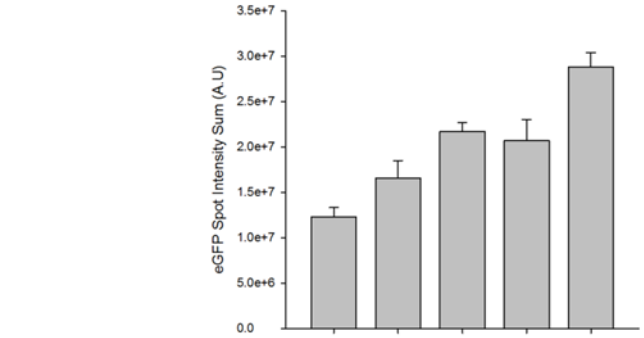

EGFR-mCherry (nM)	0.5	0.5	0.72	1.0	1.0
Wild-type HER2-eGFP (nM)	1.07	-	-	2.14	-
S310F HER2-eGFP (nM)	-	1.49	2.14	-	2.98

Figure 11. Single-molecular interaction analysis for the S310F mutant and EGFR heterodimerization. The transfected HEK 293T cell lysates were subjected to a flow chamber coated with anti-mCherry antibody. Then, the summed intensity of eGFP spots was measured and plotted. Results represent the mean ± SD obtained from experiments performed in triplicate.

Discussion

After the initiation of the Cancer Genome Anatomy Project, new genetic alterations and new driver events were found in human cancers[53]. Somatic mutations of HER2 have been identified in a wide range of solid tumors, including breast, lung, colorectal, bladder, gastric, and cervical cancers[54-59]. HER2 activating mutations have beenidentified mostly in the kinase domain. C515R, T526A, G776R, L755S, L869R, R897G, and P1074S mutations were reported to increase phosphorylation levels of HER2. D769H and V777L mutations increased the phosphorylation of both HER2 and EGFR[26,60]. L755S and V777L were the most studied mutations in clinical cases[61,62]. Cells with HER2 L775S mutation showed increased levels of phospho-EGFR, -HER2, and -HER3[26]. Patients with the HER2 L755S mutation were resistant to trastuzumab and lapatinib treatment, and a non-small cell lung cancer patient with HER2 N813D mutations was resistant to afatinib[63,64]. HER2 positive metastatic colorectal cancer patients with HER2 T784G mutation did not respond to cetuximab therapy[65]. A recent study showed that cells with the HER2 L755S mutation were

resistant to lapatinib[66]. HER2 activating mutations were also found on the extracellular domain. Seven mutations, including G309 and S310 mutations, were found to increase the phosphorylation level of HER2 (Table 1)[31,61]. However, the mechanism of how these extracellular mutations increase the phosphorylation of HER2 has not been clarified.

In our study, ligand-independent HER2 dimerization blocking antibody, trastuzumab, did not inhibit the phosphorylation of HER2 in 5637 cells (Figure 7), although it bound to the S310F mutant as well as the wild-type HER2 (Figure 3b). Trastuzumab treatment also did not hinder the proliferation of the cells (Figure 8). This observation proved that either S310F mutant or wild-type HER2 can be activated without forming heterodimer or homodimers among the mutant and wild-type HER2. Because 5637 cells overexpress the EGFR, we hypothesized that the S310F mutant or wild-type HER2 formed heterodimers with the EGFR. As expected, the ligand binding-blocking antibody, cetuximab, almost completely abolished the phosphorylation of not only EGFR but also HER2 (Figure 7). As a ligand-dependent HER2 heterodimerization blocking antibody, pertuzumab did not inhibit the

phosphorylation of HER2 (Figure 7), while it bound to wild-type HER2 (Figure 3a), EGFR-mediated phosphorylation should occur on the S310F mutant HER2. In this study, we were unable to determine the level of wild-type and S310F mutant in 5637 cells at the protein level; however, the limited amount of wild-type HER2 compared to the S310F mutant might be the reason why pertuzumab is not effective. To determine whether the S310F mutant retained affinity for the EGFR, we performed single molecule interaction analyses using a TIRF microscope as described previously[50]. The S310F HER2 mutant showed an affinity equivalent to that of wild-type HER2 in the formation of EGFR/HER2 complexes (Figure11).

In this study, we confirmed the loss or reduction of pertuzumabreactivity to G309 and S310 mutated HER2 proteins (Figure 1a). Complementary determining region 3 (CDR3) of pertuzumab heavy chain makes hydrophobic and hydrogen bond contacts with residues K333 and H318 of HER2[9]. Therefore, mutations on G309 and S310 would induce critical structural changes on the epitope of pertuzumab. Interestingly, pertuzumab showed reduced binding activity to G309A mutated proteins but no reactivity to the G309E mutated proteins. The

loss of binding activity could be explained by the structural difference between the two mutated amino acids; alanine and glutamic acid. G309 is located close to the C299–C311 disulfide bond[67]. While both glycine and alanine have a small nonpolar side chain, the glutamic acid has a long and charged side chain, influencing the structure of the HER2 domain II by breaking the disulfide bond. This hypothesis was tested by using SDS–polyacrylamide gel electrophoresis of the mutated recombinant HER2 proteins. G309E mutated protein formed multimers in non–reducing conditions, while the wild–type and G309A mutated HER2 proteins formed monomers (Figure 1). This observation was in agreement with that of a previous study reporting that the G309E HER2 mutant formed homodimers under non–reducing conditions in SDS–polyacrylamide gel electrophoresis analysis, which could be resolved by reducing agents[19].These results indicate that the use of pertuzumab in combination with trastuzumab has no additional effect on patients with HER2 amplification if they have G309 or S310 mutations.

Our study showed that a HER2 S310F mutation inducedstructuralchangesin domain II of HER2, abolishing its

reactivity to pertuzumab, but its ability to form EGFR/HER2 dimers was not affected. HER2 heterodimerization with ligand-bound HERs was through a domain II-mediated dimerization interface[68]. In contrast, HER2 heterodimerization with ligand-free HERs may be mainly involved in domain IV[69]. After activation of EGFR, trastuzumab failed to reduce the phosphorylation level of the EGFR bound to HER2[70]. Meanwhile, pertuzumab reduced the phosphorylation level of EGFR bound to HER2[71]. The retained reactivity of S310F HER2 mutant to EGFR observed in our study suggested the unaffected structure of HER2 domain II on the interface of EGFR/HER2 heterodimer. C213, H215, and E243 residues of HER2 that are located on the top of the dimerization arm,are reported to stabilize the heterodimer by hydrogen bonding and salt bridges, and hence HER2 S310F mutation may not have affected the heterodimerization[72].

The effects of HER2 S310F dimerization with other molecules can be determined from the results of cell proliferation assays, using a combination of cetuximab and trastuzumab (Figure 7). Combination cetuximab-trastuzumab treatment reduced cell proliferation in 5637 cells, in contrast to

only cetuximab-treated cells. Because cetuximab-blocked HER2 S310F monomer can form dimers with neighboring molecules, trastuzumab can form dimers with neighboring molecules, trastuzumab can block this dimerization, resulting in reduced cell proliferation. Not only can the dimerization arm serve as a "hand" for EGFR/HER2 heterodimerization, but also for HER2/HER2 homodimerization and other HER2 heterodimerization[73,74]. Thus, the S310F mutation is expected to have no effect on any other forms of dimerization. We tried to determine how the level of homodimerization changes with the S310F mutation but did not proceed. Single-molecule interaction analysis using a TIRF microscope is a method of measuring interactions of a eGFP-labeled molecule with a mCherry-labeled molecule. To measure S310F HER2 homodimerization, two *HER2* genes with S310F mutations must be labeled with mCherry and eGFP. However, the probability that mCherry-labeled and eGFP-labeled HER2 proteins would dimerize with each other could be reduced, so the data is not reliable.

Reference

1 Shepard, H. M., Brdlik, C. M. & Schreiber, H. Signal integration: a framework for understanding the efficacy of therapeutics targeting the human EGFR family. *J. Clin. Invest.*118, 3574–3581, doi:10.1172/JCI36049 (2008).

2 Yarden, Y. & Sliwkowski, M. X. Untangling the ErbB signalling network. *Nat. Rev. Mol. Cell Biol.*2, 127–137, doi:10.1038/35052073 (2001).

3 Lemmon, M. A., Schlessinger, J. & Ferguson, K. M. The EGFR family: not so prototypical receptor tyrosine kinases. *Cold Spring Harb Perspect Biol*6, a020768, doi:10.1101/cshperspect.a020768 (2014).

4 Yarden, Y. & Pines, G. The ERBB network: at last, cancer therapy meets systems biology. *Nat. Rev. Cancer*12, 553–563, doi:10.1038/nrc3309 (2012).

5 Moasser, M. M. The oncogene HER2: its signaling and transforming functions and its role in human cancer pathogenesis. *Oncogene*26, 6469–6487, doi:10.1038/sj.onc.1210477 (2007).

6 Slamon, D. J. *et al.* Human breast cancer: correlation of

relapse and survival with amplification of the HER-2/neu oncogene. *Science*235, 177-182 (1987).

7 Ghosh, R. *et al.* Trastuzumab has preferential activity against breast cancers driven by HER2 homodimers. *Cancer Res*71, 1871-1882, doi:10.1158/0008-5472.CAN-10-1872 (2011).

8 Cho, H. S. *et al.* Structure of the extracellular region of HER2 alone and in complex with the Herceptin Fab. *Nature*421, 756-760, doi:10.1038/nature01392 (2003).

9 Franklin, M. C. *et al.* Insights into ErbB signaling from the structure of the ErbB2-pertuzumab complex. *Cancer Cell*5, 317-328 (2004).

10 Agus, D. B. *et al.* Targeting ligand-activated ErbB2 signaling inhibits breast and prostate tumor growth. *Cancer Cell*2, 127-137 (2002).

11 Mann, M. *et al.* Targeting cyclooxygenase 2 and HER-2/neu pathways inhibits colorectal carcinoma growth. *Gastroenterology*120, 1713-1719, doi:10.1053/gast.2001.24844 (2001).

12 Burris, H. A., 3rd *et al.* Phase II study of the antibody drug conjugate trastuzumab-DM1 for the treatment of

human epidermal growth factor receptor 2 (HER2)-positive breast cancer after prior HER2-directed therapy. *J Clin Oncol*29, 398-405, doi:10.1200/JCO.2010.29.5865 (2011).

13 Goss, P. E. *et al.* Adjuvant lapatinib for women with early-stage HER2-positive breast cancer: a randomised, controlled, phase 3 trial. *Lancet. Oncol.*14, 88-96, doi:10.1016/S1470-2045(12)70508-9 (2013).

14 Kelly, K. *et al.* Adjuvant Erlotinib Versus Placebo in Patients With Stage IB-IIIA Non-Small-Cell Lung Cancer (RADIANT): A Randomized, Double-Blind, Phase III Trial. *J Clin Oncol*33, 4007-4014, doi:10.1200/JCO.2015.61.8918 (2015).

15 Chan, A. *et al.* Neratinib after trastuzumab-based adjuvant therapy in patients with HER2-positive breast cancer (ExteNET): a multicentre, randomised, double-blind, placebo-controlled, phase 3 trial. *Lancet. Oncol.*17, 367-377, doi:10.1016/S1470-2045(15)00551-3 (2016).

16 Connell, C. M. & Doherty, G. J. Activating HER2 mutations as emerging targets in multiple solid cancers.

*ESMO Open*2, e000279, doi:10.1136/esmoopen-2017-000279 (2017).

17 Kiss, B. *et al.* Her2 alterations in muscle-invasive bladder cancer: Patient selection beyond protein expression for targeted therapy. *Sci. Rep.*7, 42713 (2017).

18 Chumsri, S. *et al.* Prolonged Response to Trastuzumab in a Patient With HER2-Nonamplified Breast Cancer With Elevated HER2 Dimerization Harboring an ERBB2 S310F Mutation. *J. Natl. Compr. Canc. Netw.*13, 1066-1070 (2015).

19 Greulich, H. *et al.* Functional analysis of receptor tyrosine kinase mutations in lung cancer identifies oncogenic extracellular domain mutations of ERBB2. *Proc. Natl. Acad. Sci.*109, 14476-14481, doi:10.1073/pnas.1203201109 (2012).

20 Ding, L. *et al.* Somatic mutations affect key pathways in lung adenocarcinoma. *Nature*455, 1069-1075, doi:10.1038/nature07423 (2008).

21 Jia, Y. *et al.* Successful treatment of a patient with Li-Fraumeni syndrome and metastatic lung adenocarcinoma

harboring synchronous EGFR L858R and ERBB2 extracellular domain S310F mutations with the pan-HER inhibitor afatinib. *Cancer Biol. Ther.*15, 970-974, doi:10.4161/cbt.29173 (2014).

22 Eng, J. *et al.* Outcomes of chemotherapies and HER2 directed therapies in advanced HER2-mutant lung cancers. *Lung Cancer*99, 53-56, doi:10.1016/j.lungcan.2016.05.030 (2016).

23 Kan, Z. *et al.* Diverse somatic mutation patterns and pathway alterations in human cancers. *Nature*466, 869-873, doi:10.1038/nature09208 (2010).

24 Shah, S. P. *et al.* The clonal and mutational evolution spectrum of primary triple-negative breast cancers. *Nature*486, 395-399, doi:10.1038/nature10933 (2012).

25 Banerji, S. *et al.* Sequence analysis of mutations and translocations across breast cancer subtypes. *Nature*486, 405-409, doi:10.1038/nature11154 (2012).

26 Bose, R. *et al.* Activating HER2 mutations in HER2 gene amplification negative breast cancer. *Cancer Discov.*3, 224-237, doi:10.1158/2159-8290.CD-12-0349 (2013).

27 Ross, J. S. *et al.* Relapsed classic E-cadherin (CDH1)-mutated invasive lobular breast cancer shows a high frequency of HER2 (ERBB2) gene mutations. *Clin. Cancer Res.*19, 2668-2676, doi:10.1158/1078-0432.CCR-13-0295 (2013).

28 Ali, S. M. *et al.* Response of an ERBB2-mutated inflammatory breast carcinoma to human epidermal growth factor receptor 2-targeted therapy. *J. Clin. Oncol.*32, e88-91, doi:10.1200/JCO.2013.49.0599 (2014).

29 Endo, Y. *et al.* HER2 mutation status in Japanese HER2-positive breast cancer patients. *Breast Cancer*23, 902-907, doi:10.1007/s12282-015-0659-y (2016).

30 Jasra, S., Opyrchal, M., Norton, L. & Mehta, R. A Rare Case of S310F Somatic ERBB2 Mutation in a HER2-Nonamplified Breast Cancer. *Clin. Breast Cancer*17, e37-e41, doi:10.1016/j.clbc.2016.08.001 (2017).

31 Ross, J. S. *et al.* A high frequency of activating extracellular domain ERBB2 (HER2) mutation in micropapillary urothelial carcinoma. *Clin. Cancer. Res.*20, 68-75, doi:10.1158/1078-0432.CCR-13-1992 (2014).

32 Vornicova, O. *et al.* Treatment of metastatic extramammary Paget's disease associated with adnexal adenocarcinoma, with anti-HER2 drugs based on genomic alteration ERBB2 S310F. *Oncologist*19, 1006-1007, doi:10.1634/theoncologist.2014-0054 (2014).

33 Barretina, J. *et al.* The Cancer Cell Line Encyclopedia enables predictive modelling of anticancer drug sensitivity. *Nature*483, 603-607, doi:10.1038/nature11003 (2012).

34 Wang, T. *et al.* HER2 somatic mutations are associated with poor survival in HER2-negative breast cancers. *Cancer Sci*108, 671-677, doi:10.1111/cas.13182 (2017).

35 Muzny, D. M. *et al.* Comprehensive molecular characterization of human colon and rectal cancer. *Nature*487, 330-337, doi:10.1038/nature11252 (2012).

36 Han, S. W. *et al.* Targeted sequencing of cancer-related genes in colorectal cancer using next-generation sequencing. *PLoS One*8, e64271, doi:10.1371/journal.pone.0064271 (2013).

37 Wang, K. *et al.* Exome sequencing identifies frequent mutation of ARID1A in molecular subtypes of gastric

cancer. *Nat. Genet.*43, 1219-1223, doi:10.1038/ng.982 (2011).

38 Petrelli, F. *et al.* Clinical and pathological characterization of HER2 mutations in human breast cancer: a systematic review of the literature. *Breast Cancer Res. Treat*166, 339-349, doi:10.1007/s10549-017-4419-x (2017).

39 Cerami, E. *et al.* The cBio cancer genomics portal: an open platform for exploring multidimensional cancer genomics data. *Cancer Discov*2, 401-404, doi:10.1158/2159-8290.CD-12-0095 (2012).

40 Gao, J. *et al.* Integrative analysis of complex cancer genomics and clinical profiles using the cBioPortal. *Sci Signal*6, pl1, doi:10.1126/scisignal.2004088 (2013).

41 Lee, Y., Kim, H. & Chung, J. An antibody reactive to the Gly63-Lys68 epitope of NT-proBNP exhibits O-glycosylation-independent binding. *Exp. Mol. Med.*46, e114, doi:10.1038/emm.2014.57 (2014).

42 Park, S., Lee, D. H., Park, J. G., Lee, Y. T. & Chung, J. A sensitive enzyme immunoassay for measuring cotinine in passive smokers. *Clin. Chim. Acta.*411, 1238-1242, doi:10.1016/j.cca.2010.04.027 (2010).

43 Takeshi, K., Hitomi, S., Yasuto, A. & Shun'ichiro, T. *In situ* delivery and production system of trastuzumab scFv with *Bifidobacterium*. *Biochem. Biophy. Res. Commun.*493, 306-312 (2017).

44 Vajihe, A., Hamid, M. M. S., Abbas, J., Daryoush, A. & C. Perry, C. Functional expression of a single-chain antibody fragment against human epidermal growth factor receptor 2 (HER2) in *Escherichia coli*. *J. Ind. Microbiol. Biotechnol.*41, 947-956, doi:10.1007/s10295-014-1437-0 (2014).

45 Judith, N. *et al.* Novel EGFR-specific immunotoxins based on panitumumab and cetuximab show in vitro and ex vivo activity against different tumor entities. *J.Cancer. Res. Clin. Oncol*141, 2079-2095, doi:10.1007/s00432-015-1975-5 (2015).

46 Baldi, L. *et al.* Transient gene expression in suspension HEK-293 cells: application to large-scale protein production. *Biotechnol. Prog.*21, 148-153, doi:10.1021/bp049830x (2005).

47 Yoon, S. *et al.* Bispecific Her2 x cotinine antibody in combination with cotinine-(histidine)2-iodine for the

pre-targeting of Her2-positive breast cancer xenografts. *J. Cancer Res. Clin. Oncol.*140, 227-233, doi:10.1007/s00432-013-1548-4 (2014).

48 Kim, H. *et al.* Preclinical development of a humanized neutralizing antibody targeting HGF. *Exp. Mol. Med.*49, e309 (2017).

49 Lee, S. *et al.* An antibody to the sixth Ig-like domain of VCAM-1 inhibits leukocyte transendothelial migration without affecting adhesion. *J. Immunol.*189, 4592-4601 (2012).

50 Lee, H. W. *et al.* Real-time single-molecule coimmunoprecipitation of weak protein-protein interactions. *Nat. Protoc.*8, 2045-2060, doi:10.1038/nprot.2013.116 (2013).

51 Roy, R., Hohng, S. & Ha, T. A practical guide to single-molecule FRET. *Nat. Methods*5, 507-516, doi:10.1038/nmeth.1208 (2008).

52 Selvin, P. R. & Ha, T. *Single-Molecule Techniques: A Labatory Manual*. (2008).

53 Strausberg, R. L. *Cancer Genome Anatomy Project*. (Wiley Online Library, 2006).

54 Shigematsu, H. *et al.* Somatic mutations of the HER2 kinase domain in lung adenocarcinomas. *Cancer Res.*65, 1642-1646, doi:10.1158/0008-5472.CAN-04-4235 (2005).

55 Weinstein, J. N. *et al.* Comprehensive molecular characterization of urothelial bladder carcinoma. *Nature*507, 315-322, doi:10.1038/nature12965 (2014).

56 Wen, W. *et al.* Mutations in the Kinase Domain of the HER2/ERBB2 Gene Identified in a Wide Variety of Human Cancers. *J. Mol. Diagn.*17, 487-495, doi:10.1016/j.jmoldx.2015.04.003 (2015).

57 Zuo, W. J. *et al.* Dual Characteristics of Novel HER2 Kinase Domain Mutations in Response to HER2-Targeted Therapies in Human Breast Cancer. *Clin. Cancer Res.*22, 4859-4869, doi:10.1158/1078-0432.CCR-15-3036 (2016).

58 Kavuri, S. M. *et al.* HER2 activating mutations are targets for colorectal cancer treatment. *Cancer Discov.*5, 832-841, doi:10.1158/2159-8290.CD-14-1211 (2015).

59 Xiang, L. *et al.* ERBB2 mutation: A promising target in non-squamous cervical cancer. *Gynecol. Oncol.*148,

311-316, doi:10.1016/j.ygyno.2017.12.023 (2018).

60 Wang, T. *et al.* HER2 somatic mutations are associated with poor survival in HER2-negative breast cancers. *Cancer Sci.*108, 671-677, doi:10.1111/cas.13182 (2017).

61 Endo, Y. *et al.* HER2 mutation status in Japanese HER2-negative breast cancer patients. *Jpn. J. Clin. Oncol.*44, 619-623, doi:10.1093/jjco/hyu053 (2014).

62 Weigelt, B. & Reis-Filho, J. S. Activating mutations in HER2: neu opportunities and neu challenges. *Cancer Discov.*3, 145-147, doi:10.1158/2159-8290.CD-12-0585 (2013).

63 Kancha, R. K. *et al.* Differential sensitivity of ERBB2 kinase domain mutations towards lapatinib. *PLoS One*6, e26760, doi:10.1371/journal.pone.0026760 (2011).

64 Park, C. K. *et al.* Efficacy of Afatinib in a Previously-Treated Patient with Non-Small Cell Lung Cancer Harboring HER2 Mutation: Case Report. *J Korean Med Sci*33, e7, doi:10.3346/jkms.2018.33.e7 (2018).

65 Gharib, E. *et al.* HER2+ mCRC patients with exon 20 R784G substitution mutation do not respond to the

cetuximab therapy. *J. Cell Physiol*, doi:10.1002/jcp.27984 (2018).

66 Zabransky, D. J. *et al.* HER2 missense mutations have distinct effects on oncogenic signaling and migration. *Proc. Natl. Acad. Sci.*112, E6205-6214, doi:10.1073/pnas.1516853112 (2015).

67 Garrett, T. P. *et al.* The crystal structure of a truncated ErbB2 ectodomain reveals an active conformation, poised to interact with other ErbB receptors. *Mol. Cell.*11, 495-505 (2003).

68 Kumagai, T. *et al.* Role of extracellular subdomains of p185c-neu and the epidermal growth factor receptor in ligand-independent association and transactivation. *Proc Natl Acad Sci U S A*100, 9220-9225, doi:10.1073/pnas.1633546100 (2003).

69 Junttila, T. T. *et al.* Ligand-independent HER2/HER3/PI3K complex is disrupted by trastuzumab and is effectively inhibited by the PI3K inhibitor GDC-0941. *Cancer Cell*15, 429-440 (2009).

70 Maadi, H., Nami, B., Tong, J., Li, G. & Wang, Z. The effects of trastuzumab on HER2-mediated cell signaling

in CHO cells expressing human HER2. *BMC Cancer*18, 238, doi:10.1186/s12885-018-4143-x (2018).

71 Laux, I., Jain, A., Singh, S. & Agus, D. B. Epidermal growth factor receptor dimerization status determines skin toxicity to HER-kinase targeted therapies. *Br J Cancer*94, 85-92, doi:10.1038/sj.bjc.6602875 (2006).

72 Arkhipov, A., Shan, Y., Kim, E. T., Dror, R. O. & Shaw, D. E. Her2 activation mechanism reflects evolutionary preservation of asymmetric ectodomain dimers in the human EGFR family. *Elife*2, e00708, doi:10.7554/eLife.00708 (2013).

73 Hu, S. *et al.* Molecular architecture of the ErbB2 extracellular domain homodimer. *Oncotarget*6, 1695-1706, doi:10.18632/oncotarget.2713 (2015).

74 Banappagari, S., Corti, M., Pincus, S. & Satyanarayanajois, S. Inhibition of protein-protein interaction of HER2-EGFR and HER2-HER3 by a rationally designed peptidomimetic. *J Biomol Struct Dyn*30, 594-606, doi:10.1080/07391102.2012.687525 (2012).

국문초록

HER2의 도메인 2에 위치한 G309와 S310은 수용기 활성화 돌연변이로 S310F 돌연변이를 가지는 환자들은 HER2의 증폭 없이도 암을 발생시킨다고 알려져 있다.

이 연구에서는 HER2 도메인 2에 위치하며 활성화 돌연변이로 알려진 G309A, G309E, S310F, S310Y가 HER2의 세포 밖의 도메인에 결합하는 트라스투주맙과 퍼투주맙 항체와의 결합에 어떠한 영향을 미치는지 확인하였다. 먼저, ELISA로 결합력을 확인한 결과, 돌연변이가 있는 HER2 단백질에는 도메인 4에 항원결정기를 가지는 트라스투주맙 항체가 결합을 하였지만, HER2 도메인 2에 항원결정기를 가지는 퍼투주맙 항체의 경우 G309A 돌연변이를 가지는 HER2에만 결합을 하였다. 세포 표면에서의 HER2 도메인 2 돌연변이에 의한 영향을 확인하기 위하여 5637 이라는 HER2의 S310이 페닐알라닌으로 돌연변이가 생기고 EGFR이 과발현 되어있는 방광암 세포주를 찾아 연구하였다. 리간드-독립적 HER2 동형이량체 결합을 막는 트라스투주맙 항체는 5637 세포주에 발현되어있는 HER2 수용기 활성을 억제하지 못하였다. 반면, EGFR에 결합하는 세툭시맙 항체와 TKI (tyrosine kinase inhibitor)인 제피티닙에 의하여 HER2의 인산화가 감소되었고 성장이 크게 줄어들었다. 이는

5637 세포주에 존재하는 HER2가 주로 과발현 되어있는 EGFR과 이형이량체 결합을 형성하고 있다고 예상할 수 있다.S310F 돌연변이가 HER2가 EGFR과의 이형이량체 결합력에 영향을 미치지 않는다는 것을 확인하기 위하여 TIRF microscope 실험을 진행하였고, 이를 통하여 S310F 돌연변이를 가지는 HER2와 돌연변이를 가지지 않는 야생형 HER2는 EGFR와의 이형이량체 결합 정도와 비슷하다는 것을 확인하였다.

위의 연구를 통하여 S310F 돌연변이를 가지는 HER2는 문제없이 EGFR과 이형이량체 결합을 하여 활성화 되었으며, 이는 HER2에 결합하는 트라스투주맙과 퍼투주맙 항체에 의하여 억제할 수 없다는 것을 확인하였다. 이 결과는 S310F 돌연변이를 가지는 HER2가 발현 되어있고 EGFR이 과발현 되어있는 암을 가지는 환자들의 항체와 TKI 치료에 가이드라인을 제시할 수 있을 것이라고 예상된다.

주요어: HER2, 돌연변이, 퍼투주맙, 전반사 현미경, EGFR, 이형이량체 결합

학번: 2013-31177